Structural Integrity of Energy Devices Through Replica-based Microscopy and Finite Element Analysis

Subhan Ali Jogi[1,*], Muhammad Fahad Riaz[2], Ghulam Sarwar Chandio[1], Shah Behram Jitla[1], Sufyan Naseem[1],

[1]Department of Metallurgy and Materials Engineering, DUET, Karachi, Pakistan
[2]Department of Industrial Engineering and Management, DUET, Karachi, Pakistan
[*]Corresponding author: Subhan.jogi @duet.edu.pk

Abstract

Cracks and mechanical defects are very common in the service of engineering structures. In dynamic loading, the defects and scratches may turn into propagating cracks owing to stress concentration around these areas. Surface replica is applied to surface discontinuities for understanding the stress concentration factors. Replicated samples have been transformed into CAD models through the Faro Arm. The CAD model was used in a finite element model to evaluate the stress concentration factor (Kt) and the corresponding reduction of the factor of safety of structural components. It was found that the technique is extremely powerful for the prediction of the residual life of components and structures with surface damage.

Keywords—Replica; Finite Element Modelling; Corrosion; In-service damage; Stress Concentration Factor

1 Introduction

The finite element Analysis (FEA) is a problem-solving approach to identify technical issues in engineering to apply the simulation and mathematical modelling[1]. It involves the matrix in algebraic expressions for finding out the exact values of variables in a system of simultaneous linear equations and partial differentiations for structural analysis of the materials[2]. Finite Element Analysis is a software-based tool to investigate surface and subsurface defects and discontinuities within components in design or in services. Computer-Aided Design (CAD) is used to design and scrutinise data; however, Finite Element Analysis (FEA) applies numerical values to explore structural damage identification of engineering structures under loading conditions. Surface replica methods are gaining importance in non-destructive examination to monitor the initiation and propagation of cracks in structural components [3, 4]. The replication technique involves copying of areacific surfaces of the components damaged, where destructive testing or sample extraction is difficult to operate [5]. Nevertheless, no other technique can be utilized to investigate the surface measurements of the area of interest, whereas other similar destructive and nondestructive methods use the specimen in the grip of the testing equipment. The silicone-based rubber materials are relatively new and are significantly used in the mechanical, materials, and civil engineering structural appliances for finding out the root cause of failure [6]. The RepliSet is applied on the surface of the material and allowed it time to set according to the target surface before removing the replication from the surface of the structural material[7]. In the replication technique, an exact mirror impression of the target material is copied on the RepliSet for further laboratory inspections[8]. The replica method is exceptionally straightforward, cheap, and fast to operate for image analysis. [9]. The replication procedure provides significant advantages over other conventional measurement techniques, such as a permanent record of the specimens, better resolution, higher magnification, no contamination of polishing, and measurement opportunities in the laboratory[10]. The cracks and mechanical defects are common in the service life of engineering structures[11]. In dynamic loading, such as fatigue, these defects and scratches may turn into propagating cracks owing to stress concentration around these areas[12]. The fracture

ISSN: 2523-0379 (Online), ISSN: 1605-8607 (Print)
DOI: https://doi.org/10.52584/QRJ.2302.02

mechanics approach can be applied to identify the crack initiation and to predict the endurance limit of the 'damages' in structures[13]. However, not all discontinuities within the materials initiate the cracks; in many cases, damage observed without propagating the cracks, such as scratches, dents, gouges, corrosion pits, occurs on the surfaces of wind turbine blades, high-rise towers, shafts, bearings, and many more [14]. Only those damages initiate the cracks in which the associated stress concentration exceeds the maximum allowable stress of the material and disagree with safety factors[15]. The stress concentration around the particular arena exceeds the theoretical strength of the materials, causing catastrophic failure in early stages of the components in service. However, identification of the stress concentration factor around the specific area is not very straightforward[16]. In many cases, the damages are in very complex geometry, and the empirical relationship does not originate from the area. There are very few studies about this important area of fractured mechanics. In this study, a demonstration of the calculation of stress concentration factors from complex shapes of damage and surfaces is presented. Replica was used on the surface of different damage regions to obtain the geometries[17]. The replica samples were transformed into a CAD model through the Faro Arm[18]. The CAD model was used in the finite element method to determine the stress concentration factor (Kt) and corresponding reduction in the factor of safety of structures[19].

2 Experimental Analysis in Detail

2.1 Replica Measurement

In the replication procedure, a silicone-based rubber material of Zharmeck is used. The Zharmeck "ZETA FLOW" is a three-part silicone-based rubber material that provides excellent surface finish and the possibility of low shrinkage after curing. Replica materials are widely applied in biomedical and engineering applications for the prediction of disorders in the human body and the materials. The RepliSet is easy to apply, possesses high viscosity, and is applicable in different environmental conditions. The RepliSet is pasted on stress concentration regions at standard temperature and pressure, holding it for some period for curing purposes. Afterwards, samples are collected and wrapped in polythene bags to avoid any environmental contamination, and they send them for further examination. The flow chart diagram in Fig.1 clarifies the replication processing operation.

2.2 CAD and FE-Modelling

The present research article introduces surface profiles of the replication process that were made through a 3D laser camera, shown in Fig. 3. A FARO arm-based 3D laser scanner is used for the measurements. The scanner for this purpose employed a 3D position sensor with a laser pulse integrated on its tip. The scanner can be used as a robotic arm with multiple degrees of freedom. The scanner sets the intensity of the laser automatically according to the target surface and emits a laser beam, which is reflected from the surface. The time required in the reflection process is used to calculate the distance between the target surface and the FARO arm. This distance is then added to the position given by a 3D position sensor. The resultant surface is then generated by using a triangular mesh pattern. The surface obtained can be exported in many formats like igs, iges , step, jpg etc. with the software. In this study, the "iges" file format was used, which generates the rectangular x, y, z coordinates of each node of the surface. The finite element model was established in the industrial finite element code ABAQUS[20]. The data generated by the laser camera was transferred to the finite element model. The Python script of the finite element model was modified with the data obtained from the CAD model. 3. RESULTS and Discussion In this study, the replica was used on fracture surfaces, corrosion pits, and propagating cracks. The samples of corrosion pits were used to calculate stress concentration. In fracture surface analysis, ferrous and non-ferrous fractured surfaces were used for replication. Fig. 2 (a) and (b) show the Scanning Electron Microscope (SEM) image of a broken part and its replica. There was almost no difference in the fracture surface of the original sample and the replica measurement. It was found that the replication capability of the material was similar for the ferrous and non-ferrous. A similar result was found for polymer, glass, and ceramic materials.

Fig. 3 (a) and (b) show a metallic roller used in the sugar industry and an SEM image of a replica sample of its eroded region. The roller surface was affected by corrosion, leading to surface erosion. The functionality of the roller was affected due to this, and some cracks also started to initiate from the erosions in service life. However, some regions showed no such cracking. Hence, replica measurements were carried out on the surface to observe the geometric features of these complex eroded regions. Several complex-shaped sub geometries inside the eroded region. Some sub geometries can be seen with very small but sharp radii around their roots. It was practically impossible

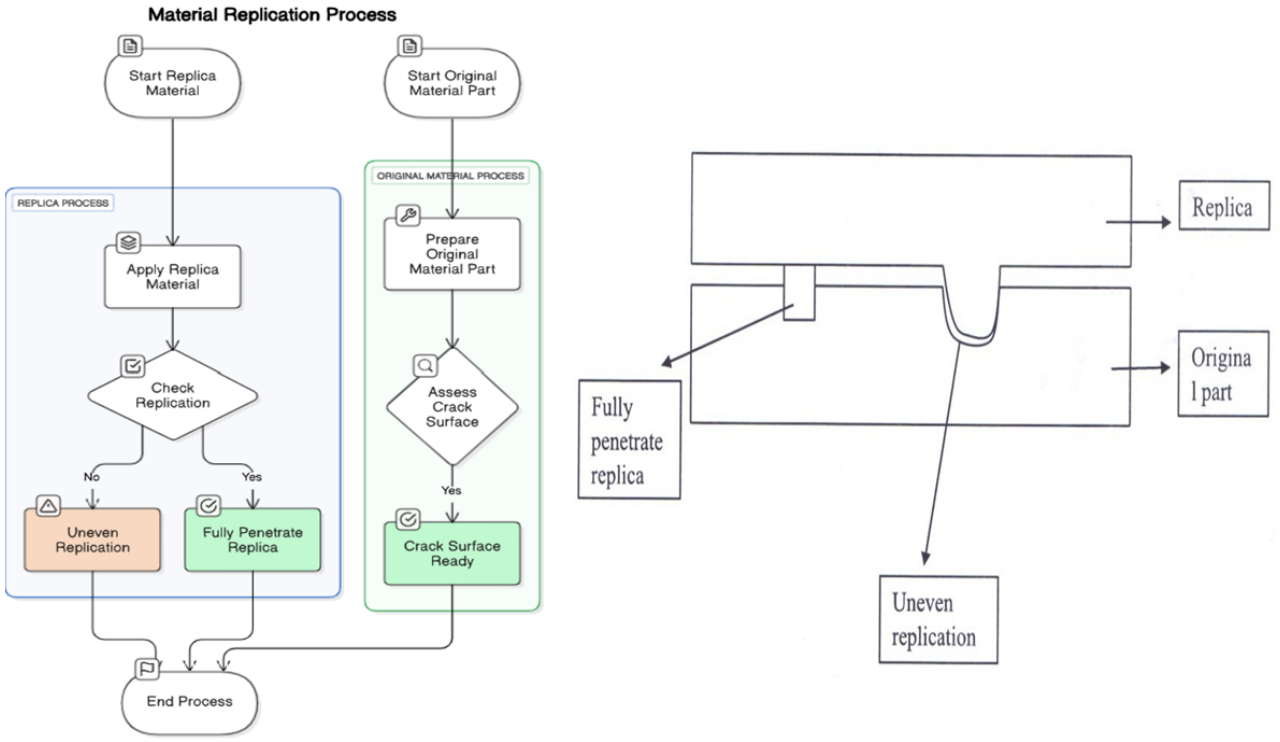

Fig. 1: Schematic illustration of the surface replication process

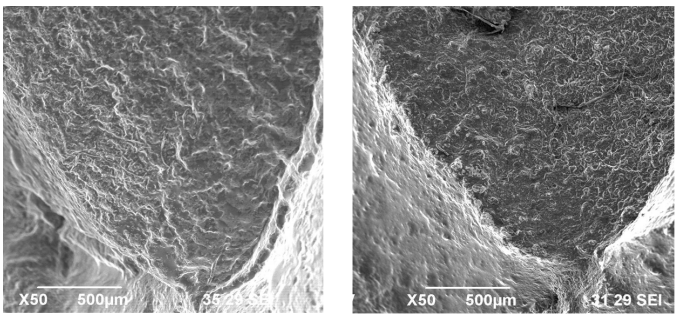

(a) original surface (b) replica surface

Fig. 2: SEM image of fracture surface

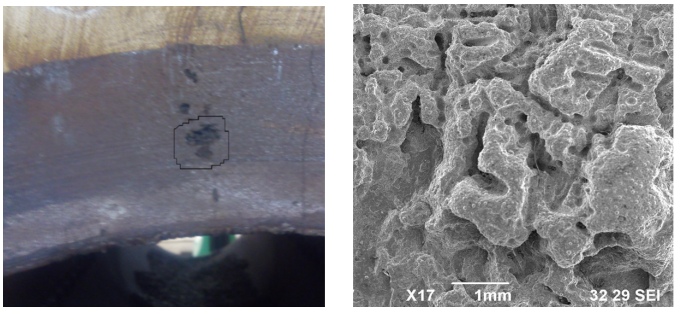

(a) Eroded surface of roller (b) complex subgeometries

Fig. 3: SEM image of replica surface

to calculate the stress concentration of such complex shapes.

3 Corrosion Pitting and Finite Element Analysis

Here, we discuss the application of a replica on a refinery vessel. The vessel was affected by corrosion pitting, leading to severe erosion on the internal walls. Replica material was applied on the inner wall of the vessel as shown in Fig. 4 (a). The replica was then taken to the laboratory, and a Faro arm was used to obtain the CAD model of the replica surface. Fig. 4 (b) shows reconstructed images of the eroded surface. The CAD model was then transformed into the finite element model of the vessel through a Python script.

The finite element model of the vessel was developed in the commercial finite element code ABAQUS. The vessel was modelled as a quarter ring of height 300mm and 50mm thickness. A 3D deformable material model was used in simulations. The Von-Mises yield criterion was applied for the determination of the plastic deformation. The material was modelled as an 8-node thermally coupled brick, trilinear displacement and temperature element named C3D8T. The pressure and temperature of 20 bars and 550 0C was applied on the internal wall of the vessel. The mesh size was kept

(a) Replica measurement on the surface of the vessel

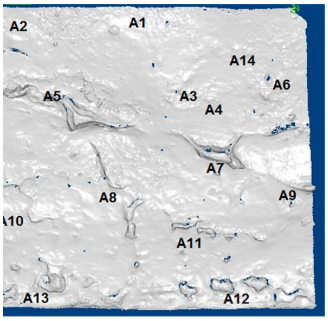

(b) CAD model of surface profile obtained from replica

Fig. 4: Replica measurement and CAD model of resultant surface profile

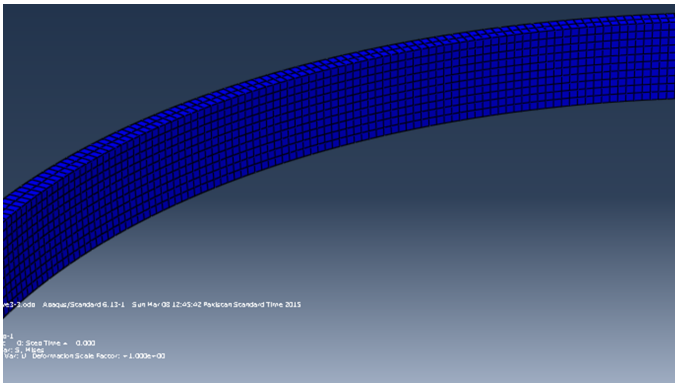

Fig. 5: Finite element model of vessel

small such that there were a total of 15000 elements in the model. Displacement boundary conditions were applied at the ends of the cylinder. A representation of the model is shown in Fig. 5. The results generated in terms of stress concentration around pitting and its effect on the factor of safety of the vessel were investigated.

Fig. 6 shows the Von-Mises stress obtained for the vessel in the presence of corrosion pits. It was found that each corrosion pit developed a very small field around its region. Around the damage zone, a very small area was affected by stress concentration. The inner wall of the ring, outside this zone, was well under those stress conditions obtained for the vessel when pitting was not considered. The maximum stress in these pits, present on the internal wall of the reactor, reached around 120MPa, like those values found at the outer wall of the vessel. It is emphasized here that without corrosion, the maximum stress at the internal wall was around 30MPa, and at the outer wall was around 100 110MPa. With these pits, the maximum stress was around 120MPa around the pits, like stress values at the outer wall of the reactor. This showed

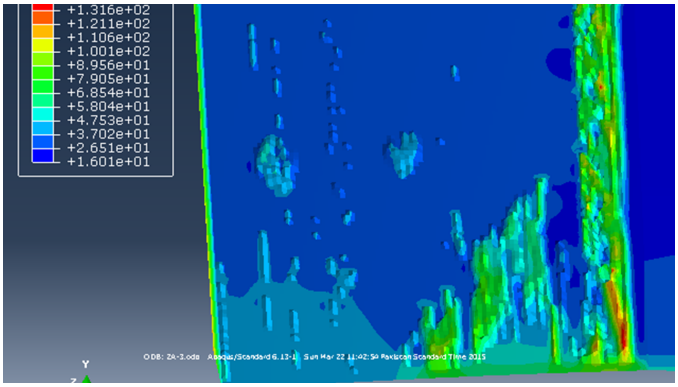

Fig. 6: Finite element model of vessel showing stress concentration around pits

that the stress concentration factor (Kt) for these pits was around 4. In addition, the stress gradient from the inner to the outer wall of the vessel was reduced. The region affected by the pitting showed that the entire 50mm thickness of the affected region showed stress of 100MPa. This showed that a safety factor of 3 was obtained here, similar to the one obtained without the corrosion pits condition.

4 Conclusion

A demonstration of a surface replica was presented to calculate the stress concentration of extremely complex shape damages. Replica samples were prepared from numerous challenging small-scale damages and observed under microscopes. The replica surfaces were used to obtain the CAD data of surfaces through the Faro Arm. The CAD data obtained from the Faro Arm was imported into the finite element method to calculate the stress concentration factor (Kt) and corresponding reduction in the factor of safety of a vessel. It was found that the technique is extremely powerful yet very straightforward for the prediction of the residual life of components and structures with surface damage.

5 Acknowledgement

The authors would like to thank the Department of Metallurgy and Materials for providing the research environment.

References

[1] R. Hashem et al., "Integrating finite element analysis and machine learning for non-invasive tumor detection: A piezoelectric tactile sensor-based vibration absorber approach," Neural Computing and Applications, pp. 1–23, 2025.

[2] V. Plevris and A. Ahmad, "Deriving analytical solutions using symbolic matrix structural analysis: Part 1—Continuous beams," arXiv preprint arXiv:2411.03514, 2024.

[3] Y. Kong, C. Bennett, and C. Hyde, "A review of non-destructive testing techniques for the in-situ investigation of fretting fatigue cracks," Materials Design, vol. 196, p. 109093, 2020.

[4] M. Civitani et al., "Evaluation of the potentialities of the roughness characterization via replica approach," in Proc. SPIE, Space Telescopes and Instrumentation 2024: Ultraviolet to Gamma Ray, 2024.

[5] M. R. Khosravani and T. Reinicke, "On the use of X-ray computed tomography in assessment of 3D-printed components," Journal of Nondestructive Evaluation, vol. 39, pp. 1–17, 2020.

[6] J. C. A. D. Filho, L. C. Nunes, and J. Xavier, "An open-source 2D digital image correlation software: Case study on the hyperelastic behaviour of silicone-based material," in Proc. Int. Conf. Testing and Experimentation in Civil Engineering, 2022.

[7] J. Perris et al., "3D printing and rapid replication of advanced numerically generated rough surface topographies in numerous polymers," Advanced Engineering Materials, vol. 25, no. 1, p. 2200832, 2023.

[8] H. M. Claypool and A. Trujillo, "Are rejection fears during interracial interactions moderated by the racial composition of the interacting partner's social network? A pre-registered replication and extension experiment," Basic and Applied Social Psychology, vol. 45, no. 1, pp. 1–12, 2023.

[9] M. Abini, "FPGA-based implementation of replica correlation using Xilinx system generator for high performance signal processing applications."

[10] B. Kohn, L. Chung, and A. Gleadow, "Fission-track analysis: Field collection, sample preparation and data acquisition," in Fission-Track Thermochronology and Its Application to Geology, 2019, pp. 25–48.

[11] L. Mishnaevsky Jr., "Repair of wind turbine blades: Review of methods and related computational mechanics problems," Renewable Energy, vol. 140, pp. 828–839, 2019.

[12] F. Xu et al., "A review of bearing failure modes, mechanisms and causes," Engineering Failure Analysis, p. 107518, 2023.

[13] Y. Ye et al., "Digital twin for the structural health management of reusable spacecraft: A case study," Engineering Fracture Mechanics, vol. 234, p. 107076, 2020.

[14] J. Aust and D. Pons, "Taxonomy of gas turbine blade defects," Aerospace, vol. 6, no. 5, p. 58, 2019.

[15] Ž. Decker et al., "Analysis of the vehicle chassis axle fractures," Materials, vol. 16, no. 2, p. 806, 2023.

[16] L. Sun and H. Niu, "A method for identifying geometrical defects and stress concentration zones in MMM technique," NDT E International, vol. 107, p. 102133, 2019.

[17] F. Bauer, M. Schrapp, and J. Szijarto, "Accuracy analysis of a piece-to-piece reverse engineering workflow for a turbine foil based on multi-modal computed tomography and additive manufacturing," Precision Engineering, vol. 60, pp. 63–75, 2019.

[18] M. Freddi et al., "Reverse engineering of a racing motorbike connecting rod," Inventions, vol. 8, no. 1, p. 23, 2023.

[19] M. Ozsoy et al., "Round bar notch shape optimization for tensile stress concentration testing," Materials Testing, vol. 65, no. 10, pp. 1551–1560, 2023.

[20] S. Ya et al., "An open-source ABAQUS implementation of the scaled boundary finite element method to study interfacial problems using polyhedral meshes," Computer Methods in Applied Mechanics and Engineering, vol. 381, p. 113766, 2021.